Network efficiency as a classifier for aging in resting state fMRI

Jaime Gomez-Ramirez, Yujie Li, Qiong Wu, Xiaoyu Tang, Jinglong Wu

Abstract Here we study how network robustness -functional network invariance under perturbation- is affected upon the removal of nodes in the functional connectivity network in resting state (R-fMRI) for both young and elder subjects. We apply analytic measures of network communication efficiency and robustness to R-fMRI in the human brain and explore the capacity of these measures to predict age. A new theoretical framework to investigate network robustness and how it is affected by internally driven processes such as aging is provided.

Key words: resting state fMRI, network degeneration hypothesis, Markov chain, relative entropy

1 Introduction

The objective of this work is to study network robustness i.e., resilience to perturbations, in resting state functional connectivity networks. It has been suggested that fluctuations in the BOLD signal measured in humans in resting state, represent the neuronal activity baseline and shape spatially consistent patterns [1], [2]. The slow fluctuations in the BOLD signal found in resting subjects, are highly coherent within either structural or functional networks in the human brain. Functional correlation based on the synchrony of low-frequency blood flow fluctuations in resting state have been identified in the sensorimotor [3], visual [4], language [5], auditory [6], dorsal and ventral attention [7] and the frontoparietal control system [8].

The visual identification of the overall connectivity patters in resting state functional magnetic resonance imaging (R-fMRI), has been assessed using either model-based and model-free approaches. In the former, statistical parametric maps of brain activation are built upon voxel-wise analysis location [9]. While this approach has been successful in the identification of motor networks [**?**], it shows important limitations when the seed voxel cannot be easily identified [10]. For example, in brain areas with unclear boundaries i.e., cognitive networks involved for instance, in memory or self processing operations [11].

Biomedical Engineering Laboratory, Okayama University, Japan

Independent Component Analysis (ICA), on the other hand, is a model-free approach that allows separating resting fluctuations from other signal variations, resulting on a collection of spatial maps, one for each independent component, that represent functionally relevant networks in the brain [12]. While ICA has the advantage over model-free methods that it does not need to assume a specific temporal model of correlation between regions of interest, the functional relevance of the different components is, however, computed relative to their resemblance to a number of networks based on criteria that are not easily formalized [13].

A third approach, complementary to the other two, which is becoming of paramount importance is the network-based approach. Graph-based techniques have proliferated in the last years providing new insights into the structure function relationship in the healthy brain, aging and neuropathological disorders [**?**], [14], [15]. The use of graph theoretic techniques to model brain networks has shifted the emphasis from the identification of local subnetworks -default mode network, primary sensory motor network etc.- to the quantitative study of the topological and informational characteristics of large-scale brain networks. Prove of the utility of this approach is that notable proponents of a modularist vision of brain connectivity to understand cognition, such as Gazzaniga [16] (see [17] for an early critic of the modularist approach by Fuster who anticipates a shift toward networks) has now embraced a complex brain networks approach [18].

Network-based approaches to R-fMRI data have demonstrated non-trivial topological properties of functional networks in the human brain. Large-scale anatomical connectivity analysis in the mammalian brain, shows that brain topology is neither random nor regular. Instead, small world architectures [19] -highly clustered nodes connected thorough relatively short paths- have been identified in brain networks. Small world networks are not solely structural, functional networks with a small world organization have been identified in the mammal brain [20]. Small world network properties have also been consistently found across different conditions, including normal development, aging, and in various pathological conditions. For a review of network analysis in R-fMRI, see [14].

While network-based studies have been successful in delineating generic network properties, such as path length or clustering, additional work is needed in order to come to grips with the internal working of the systems underlying the network. Computational simulations of disruptions in the network architecture of resting state can give clues about normal development and pathological conditions. For example, Supekar and colleagues [21] have shown that the deterioration of small world properties such as the lowering of the cluster coefficient, affect local network connectivity, which in turn may work as a network biomarker for Alzheimer's disease. Abnormalities in small-worldness may also have a significant positive correlation in, for example, schizophrenia [22] and epilepsy [23]. Transport network efficiency measures have been used to study the relationsip between structural and resting state functional connectivity [24]. The effects of lesioning in white matter connections can be studied via the simulation of the removal of individual connections from the connectome. Irimia and Van Hornreport [25] using this technique have been able to delineate "a core scaffold" or white matter network connections that when disrupted show dramatic changes in the overall organization of the human connectome. A systematic study of the effects of simulated lesioning in R-fMRI is still missing. Here we provide efficiency and robustness measures at both node and network level to show that RESULTS. We further demonstrate that MORE RESULTS

The rest of paper is structured as follows. Section 2 introduces the methodology followed in the data acquisition and reconstruction, data pre-processing, and data connectivity analysis in the

young and elder conditions. Then, we build a model to study quantitatively how network robustness is affected upon the removal of nodes in the functional connectivity network in both conditions. We provide a ranking of nodes to quantify the impact of their obliteration using a network efficiency measure based on [26]. The empirical and clinical implications of the theoretical model here are described in the results section 3. The paper concludes with a discussion section 4.

2 Materials and Methods

2.1 Data acquisition

Forty-two healthy volunteers separated in two groups, young (ages 21-32; mean 22.7) and elder (ages 51-59; mean ?) took part in the fMRI experiment. All subjects had normal or corrected-to-normal vision. The study was approved by the ethics committee of Okayama University, and written informed consent was obtained before the study. All subjects were imaged using a 1.5 T Philips scanner vision whole-body MRI system (Okayama University Hospital, Okayama, Japan), which was equipped with a head coil. Functional MR images were acquired during rest when subjects were instructed to keep their eyes closed and not to think of anything in particular. The imaging area consisted of 32 functional gradient-echo planar imaging (EPI) axial slices (voxel size=3x3x4 mm3, TR=3000 ms, TE=50 ms, FA=90^{o}, 64x64 matrix) that were used to obtain T2*-weighted fMRI images in the axial plane. We obtained 176 functional volumes and excluded the first 4 scans from analysis. Before the EPI scan, a T1-weighted 3D magnetization-prepared rapid acquisition gradient echo (MP-RAGE) sequence was acquired (TR=2300 ms, TE=2.98 ms, TI=900 ms, voxel size=1x1x1 mm3).

2.2 Data preprocessing

Data were preprocessed using Statistical Parametric Mapping software SPM8 [1] and REST v1.7 [2]. To correct for differences in slice acquisition time, all images were synchronized to the middle slice. Subsequently, images were spatially realigned to the first volume due to head motion. None of the subjects had head movements exceeding 2.5 mm on any axis or rotations greater than 2.5^{o}. After the correction, the imaging data were normalized to the Montreal Neurological Institute (MNI) EPI template supplied with SPM8 (resampled to 2x2x2 mm3 voxels) [3]. In order to avoid artificially introducing local spatial correlation, the normalized images were not smoothed. Finally, the resulting data were temporally band-pass filtered (0.01-0.08 Hz) to reduce the effects of low-frequency drifts and high-frequency physiological noises [27].

[1] http://www.fil.ion.ucl.ac.uk/spm/

[2] http://restfmri.net/forum/index.php

[3] http://imaging.mrc-cbu.cam.ac.uk/imaging/Templates

2.3 Anatomical parcellation

Before whole brain parcellation, several sources of spurious variance including the estimated head motion parameters, the global brain signal and the average time series in the cerebrospinal fluid and white matter regions were removed from the data through linear regression. Then, the fMRI data were parcellated into 90 regions using an automated anatomical labeling template [28]. For each subject, the mean time series of each region was obtained by simply averaging the time series of all voxels within that region.

2.4 Brain network construction

To measure the functional connectivity among regions, we calculated the Pearson correlation coefficients between any possible pair of regional time series, and then obtained a temporal correlation matrix $(90x90)$ for each subject. We applied Fisher's r-to-z transformation to improve the normality of the correlation matrix. Then, two-tailed one-sample t-tests were performed for all the possible 4005 i.e., $\frac{90x89}{2}$ pairwise correlations across subjects to examine whether each inter-regional correlation significantly differed from zero. A Bonferroni-corrected significance level of $P < 0.001$ was further used to threshold the correlation matrix into an adjacency matrix whose element was 1 if there was significant correlation between the two brain regions and 0 otherwise. Finally, an undirected binary graph was acquired in which nodes represent brain regions and edges represent links between regions. The study of the connectivity distribution of the resulting adjacency matrix is provided in the Appendix **??**.

2.5 Network-based model on robustness

A quantitative understanding of network robustness, that is, functional network invariance under perturbation can shed light on the properties that mediate in developmental, aging and pathological processes in the human brain. In essence, robustness measures the capacity of the network to perform the same function before and after a perturbation. Perturbations are events, internal or external, that elicit a change in the network configuration. Possible perturbations are the obliteration a node and a change in the connectivity between nodes. Thus, for a given network $G(N,E)$ a perturbation δ consisting on the removal of a set of nodes M from the initial set of nodes N, transforms the initial graph $G(N,E)$ into a new graph $G(N-M,E-E(M))$, where $N-M$ is the remaining set of nodes after having deleted the set M and $E-E(M)$ is the set of edges that do not connect any of the deleted nodes in M or $E(M)$. The robustness of the new network $G(N-M,E-E(M))$ resulting of the perturbation δ can be studied as a loss in the network efficiency Σ driven by the elimination of a set of nodes M and the edges that connect them.

The efficiency of a network G, $\Sigma(G)$, is a network centrality measure that quantifies the network's reliability in transmitting information once a node or a set of nodes have being removed. One possible measure of network efficiency can be calculated using the Latora and Marchiori measure [26]. Accordingly, the efficiency ε_{ij} in the communication between any two nodes (i,j) in

a graph G is equal to the inverse of the shortest path that connects them or

$$\varepsilon_{ij} = \frac{1}{d_{ij}} \tag{1}$$

where d_{ij} is the shortest path length or the geodesic distance between nodes i and j.

The efficiency of the graph $\Sigma(G)$ is calculated as the average of the efficiency between any two nodes ε_{ij}

$$\Sigma(G) = \frac{\sum_{i\neq j\in G}\varepsilon_{ij}}{N(N-1)} = \frac{1}{N(N-1)}\frac{1}{\sum_{i\neq j\in G} d_{ij}} \tag{2}$$

where N is the number of nodes and d_{ij} is the shortest path length between nodes i and j.

Note that when there is no path that connects the nodes i and j, $d_{ij} = \infty$, and the efficiency in the communication of the two nodes is zero, $\varepsilon_{ij} = 0$.

The robustness measure, $\mathscr{R}$, is defined as the relative performance or its complementary the efficiency loss under a network insult δ, that transforms the initial network G into G^{δ}.

$$\mathscr{R}^{\delta} = \frac{\Sigma(G^{\delta})}{\Sigma(G)} \tag{3}$$

Thus, from equation 3, a network G is considered to be robust to a perturbation δ if the network efficiency $\Sigma(G)$ stays close to the original value after a perturbation, ideally $\mathscr{R}^{\delta} = \frac{\Sigma(G^{\delta})}{\Sigma(G)} = 1$.

We can, in addition to robustness and efficiency of any given graph G, calculate the information centrality C of any node i in a network G as the variation in the network efficiency caused by the removal of the edges incident in i. The centrality of a node i, C_i, is calculated as the difference between the efficiency of the original graph G with N nodes and E edges, $G(N,E)$, and the efficiency of the resulting graph $G(N,E-k_i)$ with N nodes and $E-k_i$ edges, where k_i denotes the set of edges incident to node i. Thus, the centrality of a node is a normalized measure of the loss in network efficiency caused by the isolation of a node in G.

$$C_i = \frac{\Sigma(G(N,E)) - \Sigma(G(N,E-k_i))}{\Sigma(G(N,E))} \tag{4}$$

By the same token, the information centrality of a set of nodes S can be calculated as normalized measure of the loss in network efficiency caused by the isolation of a set of nodes S in G.

$$C_S = \frac{\Sigma(G(N,E)) - \Sigma(G(N,E-k_S))}{\Sigma(G(N,E))} \tag{5}$$

3 Results

The global network efficiency for unperturbed networks is 0.3678 for young subjects and 0.1144 for elder subjects. Thus, young subjects connectivity network is three times more efficient in terms of the shortest path distance between any two nodes.

We perturb the resting state network in two ways. First, using random node deletion and second targeting specific networks. In the random node deletion case, we build a population of networks perturbed by deleting subsets of a number of nodes in all possible combinations.

For example,

The population of perturbations P which contains all possible combination of nodes that can be deleted in a graph of N nodes has as many networks as

$$|P| = \sum_{i=1}^{N} C(N,i) = \frac{N!}{(i!)(N-i)!} \tag{6}$$

For example, the population of graphs with one node removed populated by $\sum_{i=1}^{1} C(90,i)_{i=1} = \frac{90!}{(1!)(90-1)!} = 90$ networks. Similarly, the number of perturbed networks obtained by deleting two nodes contains $\sum_{i=1}^{2} C(90,i)_{i=2} = \frac{90!}{(2!)(90-2)!} = 4095$ networks.

In this population of networks P, we build a distribution of efficiency measures for both young and elder condition.

In the **young condition**, for the population of graphs with only one node removed $P_{y,90-1}$, the efficiency measure mean is 0.3506 the standard deviation is 0.0028 and the maximum efficiency is 0.3594 for the removal of node 1 or "Precental gyrus". This node is also the one with the minimum centrality 0.0230, that is, the "Precental gyrus" has very low centrality which implies that after its removal the resulting network looses minimally its efficiency. The maximum centrality value for a single node is 0.0695 for Node 74 or region "Putamen R" which has a efficiency value of 0.3423. Thus, in random targeting of one or two nodes we observe on average a lower value for efficiency but small variance in the values of efficiency. It is expected that the variation of efficiency will increase in sensitivity with the increase in the number of nodes deleted.

For the **elder condition**, maximum efficiency is also for the removal of node 1 or "Precental gyrus", with gives an efficiency value of 0.1118. The minimum efficiency is 0.0748 for the removal of node 62 which corresponds to the region "Parietal Inf R". The mean efficiency value is 0.1067 which is less than the 0.1144 for the unperturbed network. The most central node is 62 ("Parietal Inf R") with centrality value equal to 0.03462, this same node has the biggest impact on efficiency upon its removal. The less central node is node 1 "Precental gyrus" with centrality value equal to 0.0230 which also corresponds with the node with the least efficiency impact upon its removal.

3.1 Perturbation analysis with Targeted networks

Here we also perturb the resting state network in specific ways by targeting networks of interest comparing the robustness in both conditions. In [29] it was shown that focal lesions located in the precuneus, medial anterior cingulate cortex, temporo-parietal junction, or superior frontal cortex produced substantial changes in functional connectivity. We investigate whether this is also reflected in changes in the efficiency measure. In the same study, lesions to the visual or motor cortices had restricted effects on global connectivity. YOSOLO: TO REPRODUCE THIS RESULTS.

The DMN is commonly considered to consist of medial prefrontal cortex (AAL 23, 24, 25, 26), posterior cingulate cortex/precuneus (AAL 35, 36/67 68) and bilateral inferior parietal lobule

(AAL 61, 62). The removal of the DMN in young adults gives efficiency value equal to 0.2955. In the elder condition the efficiency upon the removal of the DMN is 0.0439. Thus, for young adults an attack to the DMN represents a loss of a 15 per cent in efficiency respect to the media $(1 - \frac{0.2955}{0.3506} = 0.15$, while for the elder condition, the suppression of the DMN produces a loss of 58 per cent in efficiency respect to the media, $(1 - \frac{0.0439}{0.1067} = 0.5886)$.

4 Discussion

We have analyzed the functional connectivity in resting state of both young and elder individuals. The nodes representing the ninety brain regions based on the AAL parcellation have been ranked in terms of their impact in terms of network robustness upon removal.

The first part of our study involved random node deletion constituting a population set of perturbed networks with one and two nodes deleted in all possible combinations. In the second part the study focuses on targeted removal of specific network. We study the impact on the efficiency of the resulting network by means of metrics such as efficiency and centrality. Our results expand previous works on the study of robustness of structural brain networks. Interestingly, we find that in both elder and young groups the removal of certain nodes does not necessarily triggers a decrease in network robustness, the obliteration of certain nodes may also produces a positive impact in the network function, increasing the network robustness when the node is removed. YOSOLO:IS THIS TRUE? WHICH NODES?

YOSOLO:RESULTS The functional resting state network in young adults is more robust than for elder subjects. YOSOLO:CLARIFY THIS: The young adults are more/less robust to random deletion of nodes and or to targeted removal of networks on the basis of the efficiency metric here proposed. However, young adult networks is more/less protected against nodes/networks that are highly central (centrality measure). This finding is consistent with [**?**]

The literature reviewed here suggests that graph-based network analyses are capable of uncovering system-level changes associated with different processes in the resting brain, which could provide novel insights into the understanding of the underlying physiological mechanisms of brain function. We also highlight several potential research topics in the future. Graph theory-based approaches model the brain as a complex network in which nodes represent brain regions of interest and the edges connecting nodes represent relationship between nodes e.g., functional connectivity.

For the future we expect to establish a link between pathological lesions and the topological centrality and the efficiency of nodes studied here, and replicate our results with different imaging techniques. We intend to investigate whether, as postulated in [30] hubs of human brain networks are more likely to be anatomically abnormal than non-hubs in many brain disorders.

5 Appendix

Here we combine graph and information theory based approaches to understand network robustness in resting state-fMRI (R-fMRI) Graph theory provides a theoretical framework to investigate the overall architecture of the brain. The systematic study of these patterns using correlation anal-

ysis techniques has identified a number of resting state networks, which are functionally relevant networks found in subjects in the absence of either goal directed-task or external stimuli. Until the recent advent of graph theoretic methods in R-fMRI, the focus was put on the identification of anatomically separated regions that show a high level of functional correlation during rest. The tools we use to model a system may also convey an ontological version of it, that is to say, the system under study is seen through the lens of a specific approach that necessarily shapes the observability domain. Thus, the identification of different subnetworks during rest can be seen as a by-product of the techniques used, for example identification component analysis (ICA) or clustering.

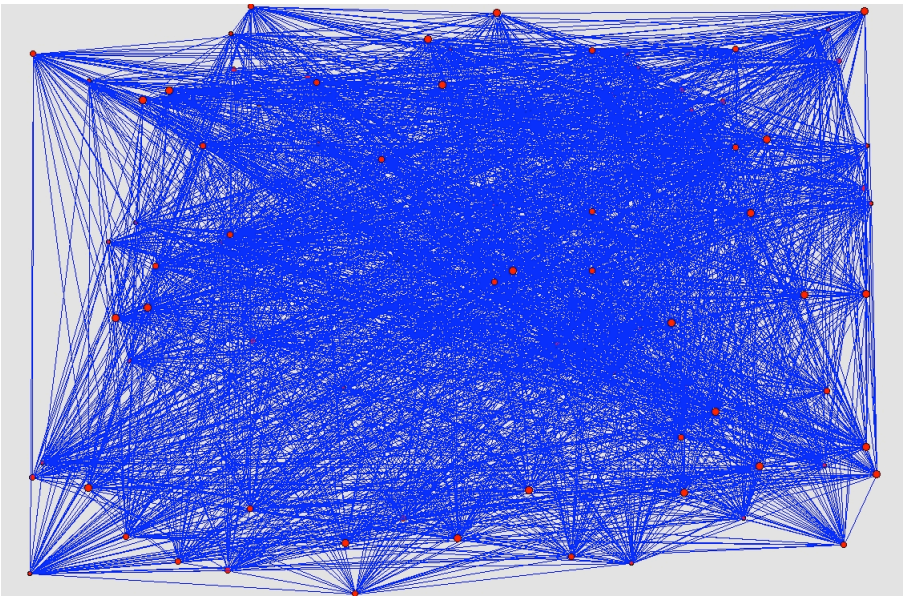

Fig. 1 Graphic representation of the functional connectivity among regions based on the temporal correlation matrix of the twenty-three healthy controls, using Pajek software [**?**]

References

1. M. E. Raichle and D. A. Gusnard, "Intrinsic brain activity sets the stage for expression of motivated behavior," *The Journal of Comparative Neurology*, vol. 493, no. 1, pp. 167–176, 2005.
2. P. Fransson, "How default is the default mode of brain function?: Further evidence from intrinsic BOLD signal fluctuations," *Neuropsychologia*, vol. 44, no. 14, pp. 2836–2845, 2006.
3. S.-M. Kokkonen, J. Nikkinen, J. Remes, J. Kantola, T. Starck, M. Haapea, J. Tuominen, O. Tervonen, and V. Kiviniemi, "Preoperative localization of the sensorimotor area using independent component analysis of resting-state fMRI," *Magnetic resonance imaging*, vol. 27, pp. 733–740, July 2009. PMID: 19110394.

4. J. S. Damoiseaux, S. A. R. B. Rombouts, F. Barkhof, P. Scheltens, C. J. Stam, S. M. Smith, and C. F. Beckmann, "Consistent resting-state networks across healthy subjects," *Proceedings of the National Academy of Sciences of the United States of America*, vol. 103, pp. 13848–13853, Sept. 2006. PMID: 16945915.
5. M. Hampson, B. S. Peterson, P. Skudlarski, J. C. Gatenby, and J. C. Gore, "Detection of functional connectivity using temporal correlations in MR images," *Human brain mapping*, vol. 15, pp. 247–262, Apr. 2002. PMID: 11835612.
6. M. D. Hunter, S. B. Eickhoff, T. W. R. Miller, T. F. D. Farrow, I. D. Wilkinson, and P. W. R. Woodruff, "Neural activity in speech-sensitive auditory cortex during silence," *Proceedings of the National Academy of Sciences of the United States of America*, vol. 103, pp. 189–194, Jan. 2006. PMID: 16371474.
7. M. D. Fox, M. Corbetta, A. Z. Snyder, J. L. Vincent, and M. E. Raichle, "Spontaneous neuronal activity distinguishes human dorsal and ventral attention systems," *Proceedings of the National Academy of Sciences of the United States of America*, vol. 103, pp. 10046–10051, June 2006. PMID: 16788060.
8. J. L. Vincent, I. Kahn, A. Z. Snyder, M. E. Raichle, and R. L. Buckner, "Evidence for a frontoparietal control system revealed by intrinsic functional connectivity," *Journal of neurophysiology*, vol. 100, pp. 3328–3342, Dec. 2008. PMID: 18799601.
9. B. Biswal, F. Z. Yetkin, V. M. Haughton, and J. S. Hyde, "Functional connectivity in the motor cortex of resting human brain using echo-planar MRI," *Magnetic resonance in medicine: official journal of the Society of Magnetic Resonance in Medicine / Society of Magnetic Resonance in Medicine*, vol. 34, pp. 537–541, Oct. 1995. PMID: 8524021.
10. J. A. Maldjian, "Functional Connectivity MR Imaging: Fact or Artifact?," *American Journal of Neuroradiology*, vol. 22, pp. 239–240, Feb. 2001.
11. A. A. Fingelkurts and A. A. Fingelkurts, "Persistent operational synchrony within brain default-mode network and self-processing operations in healthy subjects," *Brain and Cognition*, vol. 75, pp. 79–90, Mar. 2011.
12. V. D. Calhoun, J. Liu, and T. Adali, "A review of group ICA for fMRI data and ICA for joint inference of imaging, genetic, and ERP data," *NeuroImage*, vol. 45, pp. S163–172, Mar. 2009.
13. B. B. Biswal, M. Mennes, X.-N. Zuo, S. Gohel, C. Kelly, S. M. Smith, C. F. Beckmann, J. S. Adelstein, R. L. Buckner, S. Colcombe, A.-M. Dogonowski, M. Ernst, D. Fair, M. Hampson, M. J. Hoptman, J. S. Hyde, V. J. Kiviniemi, R. KÃ¶tter, S.-J. Li, C.-P. Lin, M. J. Lowe, C. Mackay, D. J. Madden, K. H. Madsen, D. S. Margulies, H. S. Mayberg, K. McMahon, C. S. Monk, S. H. Mostofsky, B. J. Nagel, J. J. Pekar, S. J. Peltier, S. E. Petersen, V. Riedl, S. A. R. B. Rombouts, B. Rypma, B. L. Schlaggar, S. Schmidt, R. D. Seidler, G. J. Siegle, C. Sorg, G.-J. Teng, J. Veijola, A. Villringer, M. Walter, L. Wang, X.-C. Weng, S. Whitfield-Gabrieli, P. Williamson, C. Windischberger, Y.-F. Zang, H.-Y. Zhang, F. X. Castellanos, and M. P. Milham, "Toward discovery science of human brain function," *Proceedings of the National Academy of Sciences of the United States of America*, vol. 107, pp. 4734–4739, Mar. 2010.
14. J. Wang, X. Zuo, and Y. He, "Graph-based network analysis of resting-state functional MRI," *Frontiers in Systems Neuroscience*, vol. 4, p. 16, 2010.
15. Y. He and A. Evans, "Graph theoretical modeling of brain connectivity," *Current opinion in neurology*, vol. 23, pp. 341–350, Aug. 2010. PMID: 20581686.
16. M. S. Gazzaniga, ed., *The New Cognitive Neurosciences: Second Edition*. The MIT Press, 2 ed., Nov. 1999.
17. J. Fuster, "The module: crisis of a paradigm book review, "the new cognitive neurosciences" 2nd edition, m.s. gazzaniga, editor-in-chief, mit press," *Neuron*, no. 26, pp. 51–53, 2000.
18. D. S. Bassett and M. S. Gazzaniga, "Understanding complexity in the human brain," *Trends in cognitive sciences*, vol. 15, pp. 200–209, May 2011. PMID: 21497128.
19. D. Watts and S. Strogatz, "Collective dynamics of 'small-world' networks," *Nature*, vol. 393, pp. 244–442, 1998.
20. D. S. Bassett and E. Bullmore, "Small-world brain networks," *The Neuroscientist*, vol. 12, pp. 512–523, Dec. 2006.
21. K. Supekar, V. Menon, D. Rubin, M. Musen, and M. D. Greicius, "Network analysis of intrinsic functional brain connectivity in alzheimer's disease," *PLoS Computational Biology*, vol. 4, June 2008. PMID: 18584043 PMCID: PMC2435273.
22. Y. Liu, M. Liang, Y. Zhou, Y. He, Y. Hao, M. Song, C. Yu, H. Liu, Z. Liu, and T. Jiang, "Disrupted small-world networks in schizophrenia," *Brain: a journal of neurology*, vol. 131, pp. 945–961, Apr. 2008. PMID: 18299296.
23. W. Liao, Z. Zhang, Z. Pan, D. Mantini, J. Ding, X. Duan, C. Luo, G. Lu, and H. Chen, "Altered functional connectivity and small-world in mesial temporal lobe epilepsy," *PLoS ONE*, vol. 5, p. e8525, Jan. 2010.

24. J. Goni, M. P. v. d. Heuvel, A. Avena-Koenigsberger, N. V. d. Mendizabal, R. F. Betzel, A. Griffa, P. Hagmann, B. Corominas-Murtra, J.-P. Thiran, and O. Sporns, "Resting-brain functional connectivity predicted by analytic measures of network communication," *Proceedings of the National Academy of Sciences*, vol. 111, pp. 833–838, Jan. 2014.
25. A. Irimia and J. D. Van Horn, "Systematic network lesioning reveals the core white matter scaffold of the human brain," *Frontiers in Human Neuroscience*, vol. 8, p. 51, 2014.
26. V. Latora and M. Marchiori, "Efficient behavior of small-world networks," *Physical Review Letters*, vol. 87, p. 198701, Oct. 2001.
27. Q. Jiao, G. Lu, Z. Zhang, Y. Zhong, Z. Wang, Y. Guo, K. Li, M. Ding, and Y. Liu, "Granger causal influence predicts BOLD activity levels in the default mode network," *Human Brain Mapping*, vol. 32, pp. 154–161, Jan. 2011.
28. N. Tzourio-Mazoyer, B. Landeau, D. Papathanassiou, F. Crivello, O. Etard, N. Delcroix, B. Mazoyer, and M. Joliot, "Automated anatomical labeling of activations in SPM using a macroscopic anatomical parcellation of the MNI MRI single-subject brain," *NeuroImage*, vol. 15, pp. 273–289, Jan. 2002.
29. J. Alstott, M. Breakspear, P. Hagmann, L. Cammoun, and O. Sporns, "Modeling the Impact of Lesions in the Human Brain," *PLoS Comput Biol*, vol. 5, p. e1000408, June 2009.
30. N. A. Crossley, A. Mechelli, J. Scott, F. Carletti, P. T. Fox, P. McGuire, and E. T. Bullmore, "The hubs of the human connectome are generally implicated in the anatomy of brain disorders," *Brain*, vol. 137, pp. 2382–2395, Aug. 2014.